Cumhuriyet Üniversitesi Fen Fakültesi
Fen Bilimleri Dergisi (CFD), Cilt:36, No: 3 Özel Sayı (2015)
ISSN: 1300-1949

Cumhuriyet University Faculty of Science
Science Journal (CSJ), Vol. 36, No: 3 Special Issue (2015)
ISSN: 1300-1949

A Double-Stator Switched Reluctance Motor for Direct-Drive Washing Machine Application

M. ASGAR[1,*], E. AFJEI[1], M. M. MAHMOODI[2], A. R. BAHRAMI[2], E. Z. ALIABADI[3]

[1] *Department of Electrical Engineering, Shahid Beheshti University, G.C., Tehran, Iran*

[2] *Department of Electrical Engineering, Saveh Branch, Islamic Azad University, Saveh, Iran*

[3] *Department of Technical and Vocational College of Islamic Enghelab, Tehran, Iran*

Received: 01.02.2015; Accepted: 05.05.2015

Abstract. Switched reluctance motors (SRMs) are known as an economical solution by several unique features such as: simple structure and low cost maintenance. Furthermore, due to the lack of permanent magnet, powerful and economical structure of these types of motors, they are proposed as a good choice for use in household appliances. In this paper, a high power flat-type double-stator SRM with low operating voltage in direct-drive system is introduced. Initially, proportional to the intended application, the acceptable attribute of SRM structure is selected, and was followed by the calculation of the motor design. Next, the magnetic characteristics are analyzed by finite element method (FEM) to determine the efficiency of the motor. Finally, the collection of experimental data is tested to confirm the calculated values and the simulation results and ensure the proper functioning of the obtained collection.

Keywords: Switched reluctance motors, finite element analysis, double-stator motors, direct-drive, washing machine.

1. INTRODUCTION

Nowadays, SRMs are used for a wide range of applications, such as aerospace industry, propulsion marine equipment, linear drivers, drilling equipment, hand tools and household appliances [1-4]. The main reasons for employing SRMs on scopes which have been mentioned above, is the low cost, the resistance to admitting error and high efficiency via variable speed [5]. Therefore, the SRMs due to the low cost and also easy access to components and electronic equipment required, is proposed as a powerful corrival for other electric motors such as induction motors, brushless DC motors, permanent magnet synchronous motors and universal motors in most applications [6-8]. In practice phase, the configuration of SRMs is supposed to be developed with the fault-tolerant on mechanical and electrical performance on washing machine application. Otherwise, if there is any weakness or defect in the motor, then SRMs technology has the potential to cover or compensate the inherit limitations by closed-loop controller circuits.

In this paper, design process of a three-phase DSSRM with 12/8 poles, (12 poles for inner stators, 12 poles for outer stators and 8 double-side poles for rotor), is proposed. Motor structure and its properties are described in Section 2. Details of the design and calculation of the frame sizing are given in Section 3.

*Corresponding author. *Email address*: *m_asgar@sbu.ac.ir*

Special Issue: The Second National Conference on Applied Research in Science and Technology

In Section 4, the equivalent model based on the calculated size, is analyzed. Also, in this study a magnetic analysis is performed in three-dimensional condition by specialized software which is called "Magnet" package [9]. In Section 5, an experimental testing and also field trail is performed on the constructed prototype. Finally, in Section 6, the summary of the obtained results are offered.

2. DESCRIBE THE STRUCTURE OF PROPOSED DSSRM

Proportional to the defined application, a DSSRM with 12/8 poles is introduced as an innovation in application. The two-side segmented rotor includes salient poles. The coils are located on both inner and outer stators poles and the poles are linked to each other by means of the yoke. The rotor places between inner and outer stators. In proposed structure of this segmented rotor, yoke is not existed so the detached parts of rotor are interrelated by thin sheets of soft magnetic materials. In proposed rotor structure, the segments of the rotor are located on a supported aluminum plate. In this structure shaft can be eliminated. Selecting such a different configuration of SRMs is customized with respect to intended application and imposed limitations such as: space restriction and obtaining the required torque generated via different speed in washing and drying cycles on washing machines application.

The wash program chosen determines the overall time period of the washing cycle [10-11]. As shown in Fig. 7, after completion of the washing cycle, the washing machine starts operation in the spin-dry cycle. The washing machine's drum accelerates to a pre-defined high speed level for a drying cycle where it remains for a short time. Then, the washing machine's drum is ordered to decelerate either to a stop or to proceed to a low speed level. Depending on the wash program chosen, this cycle might be repeated several times [12].

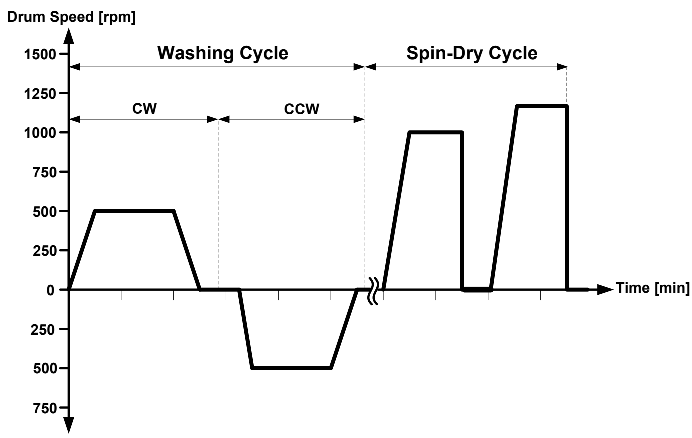

Figure 1. Washing machine operating cycles.

In SRMs, increase the number of rotor and stator poles causes the reduction of torque ripple. Instead, increasing the number of phases increases the power switches and thus, increases the cost of the motor converter. The new structure is configured in respect to these two points of view.

3. DESIGN AND CALCULATION OF THE PROPOSED SRM

In 5 Kg front-door washing machine, to evaluate the output power of its direct-drive motor, the rotor segments and drum weights are also considered in spine-dry cycle. In this case, the motor speed increases to nominal speed. In washing cycle, due to utilizing the PWM controller, the speed of the motor decreases and stabilizes under about 50 [rpm].

$$P = P_{in} + P_{out} = F \times v_m \tag{1}$$

The following equation can be used to convert the linear velocity to the angular velocity:

$$N_r = \frac{v_m}{D/2} \times \frac{60}{2\pi} \tag{2}$$

Calculating process of the parameters which are required in the design of SRMs, followed by design process of double stators SRMs based on the above computed parameters. To achieve an appropriate continuity of torque the minimum stator pole arc is calculated as follows:

$$\beta_s[\min] = \frac{4\pi}{N_s \times N_r} \tag{3}$$

This point is notable, that to achieve maximum power delivered by the motor, the stimulation phase angel must be equal to stators poles arc:

$$k_d = \frac{\theta_i \times q \times P_r}{360} \tag{4}$$

As seen in Fig. 2, the outer diameter of the inner stator of a DSSRM is calculated by output power equation as follows:

$$D_{in} = \sqrt{\frac{\pi \times P_{in}}{60 k_e k_d k_1 k_2 k B A_S v_m}} \tag{5}$$

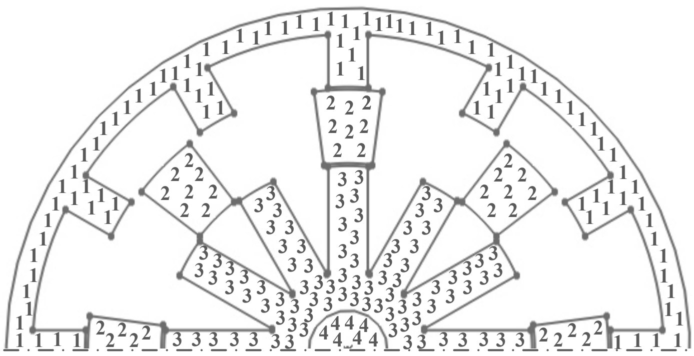

Figure 2. Cross section of a 12/8 three-phase segmented rotor DSSRM. 1-Outer stator, 2-Rotor, 3-Inner stator, 4-Shaft.

The inner diameter of the outer stator is computed by output power equation as follows:

$$D_{out} = \sqrt{\frac{\pi \times P_{out}}{60 k_e k_d k_1 k_2 k B A_S v_m}} \tag{6}$$

In practice, due to the considered limitation in design procedure of SRMs which is mentioned in section 2, and also due to the determining the standard dimensions for washing machine, the outer diameter is imposed to the assumption of the process and thus the thickness of motor is extracted from this equation:

$$L = k \times D \quad (7)$$

In SRMs the torque generated in result of the interaction between the electric and magnetic loading, so the torque produced on the middle rotor by inner stator function can be calculated by the following equation:

$$T_{in} = k_d k_e k_2 k_3 (B \times A_S) \times D_{in}^2 \times L \quad (8)$$

In general, the total output torque of the proposed DSSRM is obtained by the following equation.

$$T = T_{in} + T_{out} \quad (9)$$

Finally, according to the equation and considered washing machine application, the electrical parameters and geometrical dimensions are summarized on Table 1.

Table1. Extracted dimensions and electrical parameters of the DSSRM.

Parameter	Definition	Value	Parameter	Definition	Value
N_s	**Stator pole number**	12(dual)	P	**Elec. Input power**	1.25 [KW]
N_r	**Rotor pole number**	8	P_{out}	**Outer stator elec. power**	0.75 [KW]
q	**Phase number**	3	P_{in}	**Inner stator elec. power**	0.5 [KW]
D	**Outer diameter of the motor**	260 [mm]	T	**Total torque**	11.2 [N.m]
D_0	**Outer stator inside diameter**	200 [mm]	T_{out}	**Outer stator torque**	5.8 [N.m]
D_i	**Inner stator outside diameter**	140 [mm]	T_{in}	**Inner stator torque**	5.4 [N.m]
L	**Stack length**	40 [mm]	β_s	**Stator pole arc**	7.5 [Deg.]

4. MODELING OF THE PROPOSED DSSRM

To predict the performance of the motor, the magnetic flux distribution of the rotor is performed at different directions and also by phase stimulation of the different currents. To achieve an accurate estimation and in respect of nuclear magnetic saturation phenomenon, a powerful three-dimensional model of the motor is needed. In Fig. 3, a three-dimensional model developed by the engineering design software and tools is shown. As seen in Fig. 3, a segmented rotor is surrounded by two coaxial stators. In addition, the torque is generated on a single rotor by both inner and outer stators.

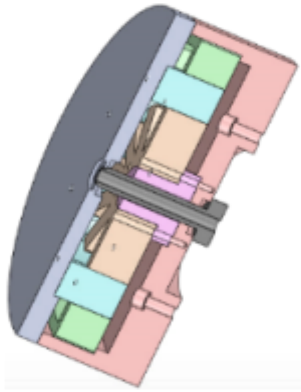

Figure 3. Primary 3-D model of DSSRM.

In general, analyzing with a 3D FEM model due to having the ability of modeling at the saturation condition, not only at the static status but also at the dynamic conditions, is an appropriate and developed tool to design the proposed motor.

Therefore, based on the calculated parameters by mathematical relations, the accuracy of the values is re-evaluated by FEM model. Separate model of proposed motor which divisions of the finite element grid is done and the extruded view is shown in Fig. 4.

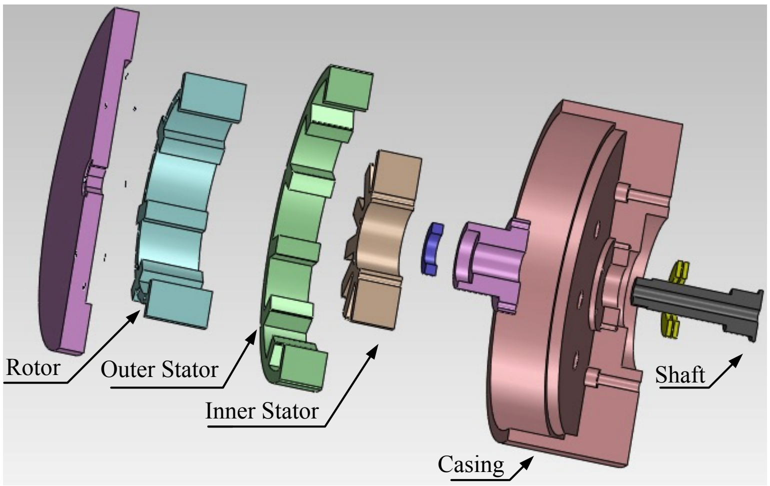

Figure 4. Extruded view of proposed DSSRM.

In addition, magnetic flux distribution in aligned and fully unaligned positions under 2[A] excitation phase current, are illustrated in Figs. 4(a) and 4(b). The maximum flux density on the surface of the rotor poles and the inner and outer stators is about 1.4 Tesla. To placing 3D coils on its stator, three-dimensional model that designed in the previous step (assembled model) will be imported to the magnetic package environment. Fig. 4 shows the model include coils realized in the simulator. As can be seen, through the adjacent stator poles, the flux vectors of the stator poles are spreading outward back to the stator yoke. In the case of 12 by 8 SRM, a rotor position of zero degrees is in aligned position (Fig. 4(a)). In against, a rotor position of 15 degrees is in unaligned position (Fig. 4(b)), just where the inductance of the phase winding is in its minimum values. The maximum flux linkage of the model is created on the rotor and stators poles edges.

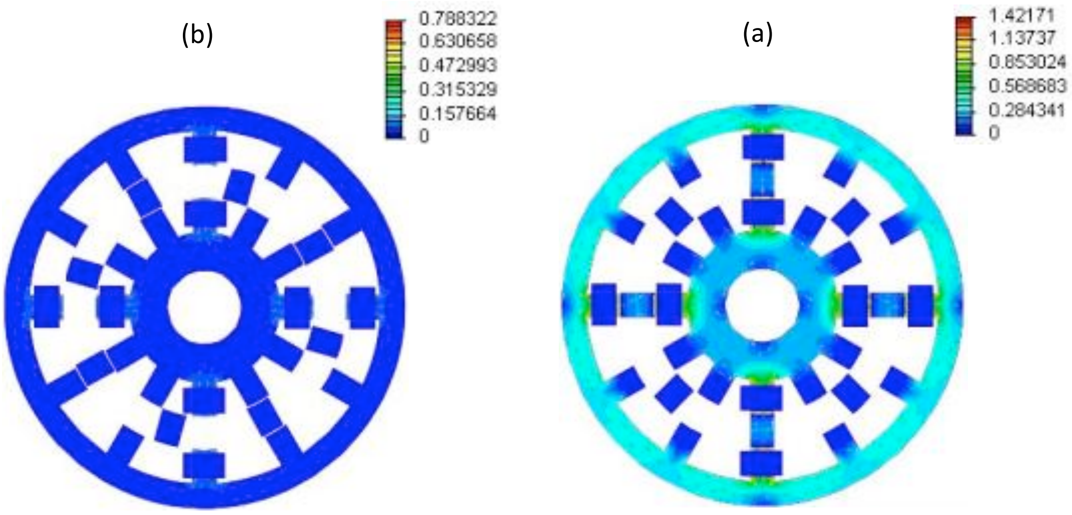

Figure 5. Magnetic flux distribution on the rotor and stators poles in a) aligned, and b) unaligned positions.

Fig.6 shows the inductance variation from unaligned to aligned positions. The minimum value of the inductance is 13[mH] in unaligned position and the maximum of the inductance is 39[mH] in aligned position. The interval between minimum and maximum values of inductance has been changed non-linearly, this deferential value of inductance amplitude helps to produce more torque. It should be noted that, the obtained result is the same as analytical design.

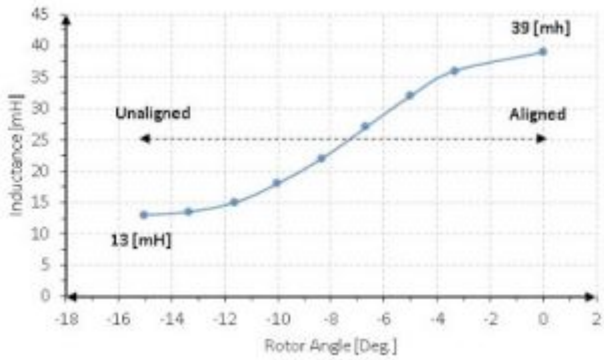

Figure 6. Flux linkage in both aligned and unaligned positions vs. different excitation current.

The obtained results of the changing trend of the co-energy under different phase current from aligned to unaligned positions in means of simulation technique by FEM is presented in Fig. 6.

As the graph clearly shows, the maximum values of phase windings co-energy are happened at aligned position. At the unaligned positions, the phase windings co-energy falls slowly to zero. The maximum values of phase windings co-energy under 2, 4, 6, 8 and 10 excitation phase currents are obtained 6, 4.37, 2.83, 1.42 and 0.36 [J] respectively.

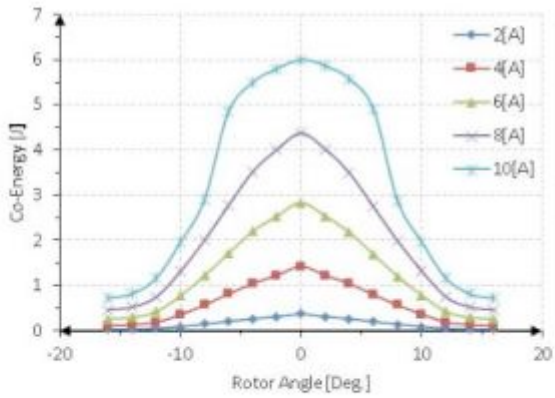

Figure 6. Simulation of co-energy vs. variation of rotor angles.

In SRMs exerted normal forces on the rotor are as a function of rotor position and the number of coils winding of the two stators. Fig. 7 shows the exerted forces at unaligned to the next unaligned position versus different phase currents. As seen in Fig. 7, in all levels of currents, the normal forces values at around the unaligned positions are equal to zero. The maximum normal forces under excitation phase currents 2, 4, 6, 8 and 10 [A] are obtained 33.7, 26.8, 19.3, 12 and 3.5 [N] respectively.

Actually, as same as the other SRMs, in the proposed DSSRM the motion forces control are performed by the controlling circuits.

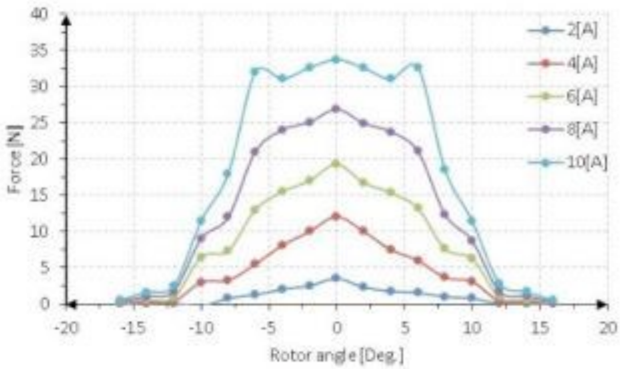

Figure 7. Torque vs. rotor position in different excitation currents.

3. IMPLEMENTATION AND EXPERIMENTAL STUDY

Different parts of the proposed DSSRM before coiling and assembling are shown in Fig. 8. The proposed motor with one rotor and two inner and outer stators are embedded on a cylindrical frame of aluminum in the form of concentric placed next to each other. The segments of the rotor are placed on an aluminum plate. In segmented rotor structure the yoke is eliminated so the weight of rotor is significantly reduced. Locating the motor shaft on one bearing is a special feature of the proposed motor. In practice, instead of shaft, washing machine drum axis is linked directly to the aluminum plate. In the proposed structure the thickness of the motor proportional to the usable space of washing machines is considered small. Therefore the proposed DSSRM is classified as a flat-type motor among the different frame size motors.

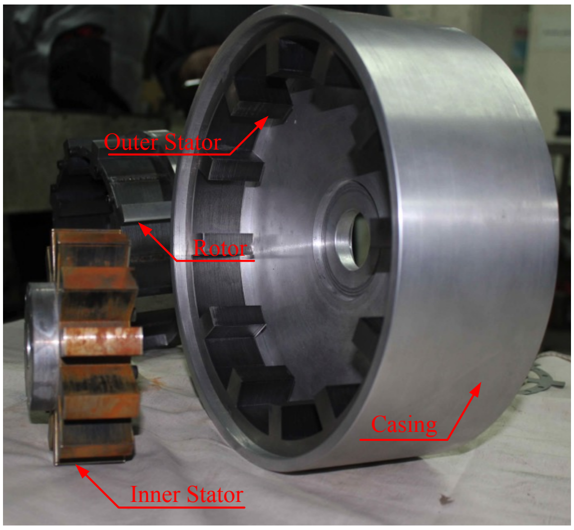

Figure 8. Different parts of proposed DSSRM before coiling and assembling.

One of the features of motor efficiency is the appropriate torque distribution by controlling circuits. In experimental trails comparing results with extracted attributes from calculation and simulation process shows that, the acceptable torque range is provided by the proposed motor for washing mashing application. The motor collection, driver & controlling circuits and required DC-Link source in test bench is shown in Fig. 9. The central core of controlling circuit is designed and constructed by a prompt processor on DSPIC technology. All of the required information for drawing torque-speed graph is extracted by connecting the motor to torque measuring equipment, and then are submitted to computer via a serial port for performing open-loop analyses.

Figure 9. Torque-Speed test bench.

Testing and extracting motor parameters is followed by conducting some field and experimental trails on prototype after installation the motor on a washing machine. In Fig. 10, the motor position on a 5Kg front-door direct-drive washing machine in both current and former state is presented. As seen in Fig. 10(a), the direct-drive DSSRM is connected to the axis drum of the washing machine. In Fig. 10(b) the former state of washing machine is showed, which is provided by a BLDC direct-drive motor.

(b) (a)

Figure 10. Front-door direct-drive washing machine includes a) Proposed DSSRM b) BLDC motor.

After placing the proposed DSSRM on front-door washing machine and defining different washing programs, some field trials is performed and the washing and drying states with laundry is investigated and is observed. During the low speed (washing cycle), around 50 [RPM], and high speed (drying cycle) means 1000 [RPM], the torque ripple reducing process is performed by popular torque ripple reduction algorithms in SRMs. In the unbalanced loading state, especially at high speed, the performance of the proposed DSSRM is considerable. As seen in Fig. 10, the outer diameter of two motors is the same.

Conventional front-door direct-drive washing machine is included BLDC motor with an exterior rotor. The proposed motor includes an inner rotor between two stators. This technique reduces the normal forces and increases the motional forces. Therefore the efficiency and torque per volume of the washing machine which is used the proposed DSSRM is improved significantly.

In Fig. 11, a 5Kg front-door direct-drive washing machine which is located the proposed DSSRM on its structure is shown.

Figure 11. Motor and driver with washing machine during the field trailing.

Based on the obtained results of field trials, the proposed motor features are listed as follow:

A) To achieve a low torque ripple which is appropriate to the motor speed-torque extracted curve proposed arrangement three-phase ratio of 12 by 8 poles is considered.
B) The frame size of proposed motor is designed and calculated for a 5Kg washing machine with direct-drive technology.
C) Due to design and construction a flat-type motor with segmented rotor, the motor weight is substantially reduced and problems related to the acceleration of the engine are also reduced.
D) By reducing flux leakage, the fundamental problems associated with mortality and motor vibration is significantly reduced.
E) Due to the low DC-Link supply voltage (80 volts), the risk of electric shock is eliminated on washing machine.
F) Reducing the cost of fabrication of a washing machine which is used the proposed motor, is another benefit of this study.

6. CONCLUSIONS

In this paper, a three-phase flat-type DSSRM with 12 by 8 poles was designed and constructed by direct-drive technology for employing on washing machines. To achieve the intended purpose, first of all, the frame size of motor is calculated, then the simulation process by FEM analysis through design of three-dimensional electromagnetic model was performed and ultimately, the prototype motor has been installed on a frame of a 5Kg front door washing machine and field trials have been conducted on the motor. Based on the extracted flux distribution curves, phase inductance, torque ripple depending on the position of the rotor and investigation of aligned to unaligned position. Comparing of extracted variables from the calculations, simulation of practical results showed that; the proposed motor enables to provide speed range and torque requirements in both washing and spinning cycles. All sections of control and maximum power tracking are fed up with 80 [V] DC-link source. So the risk of electric shock has been eliminated by means of this structure.

REFERENCES

[1] Mosallanejad, A. (2014), "Analyses of the Effect of Length Difference between Plunger and Winding on Tubular Linear Reluctance Motor Performance," International Transactions on Electrical Energy Systems, pp. n/a-n/a,
[2] Labak, A. and Kar, N. C. (2013), "Designing and Prototyping a Novel Five-Phase Pancake-Shaped Axial-Flux SRM for Electric Vehicle Application Through Dynamic FEA Incorporating Flux-Tube Modeling," IEEE Transactions on Industry Applications, vol. 49, issue 3, pp. 1276–1288.
[3] Zhang, H. Xu, W. Wang, S. et al. (2014), "Optimum Design of Rotor for High-Speed Switched Reluctance Motor Using Level Set Method," IEEE Transactions on Magnetics, under publication vol. 50, issue 2.
[4] Torkaman, H. Afjei, E. and Toulabi, M. S. (2012), "New Double-Layer-per-Phase Isolated Switched Reluctance Motor: Concept, Numerical Analysis, and Experimental Confirmation," IEEE Transactions on Industrial Electronics, vol. 59, no. 2, pp. 830-838.
[5] Jun, C. Zhiquan, D. and Rongguang, H. (2014), "Position Signal Faults Diagnosis and Control for Switched Reluctance Motor," IEEE Transactions on Magnetics, vol. 50, no. 9, pp. 1-11.
[6] Yu, Q. and Gerling, D. (2013), "Analytical Modeling of a Canned Switched Reluctance Machine with Multilayer Structure," IEEE Transactions on Magnetics, vol. 49, no. 9, pp. 5069-5082.

[7] Isfahani, A. H. and Fahimi, B. (2014), "Comparison of Mechanical Vibration between a Double-Stator Switched Reluctance Machine and a Conventional Switched Reluctance Machine," IEEE Transactions on Magnetics, vol. 50, no. 2, pp. 293-296.
[8] Da-Woon, C. Sang-In, B. and Yun-Hyun, C. (2014), "A Study on the Maximum Power Control Method of Switched Reluctance Generator for Wind Turbine," IEEE Tran. On Magnetics, vol. 50, no. 1, pp. 1-4.
[9] Magnet CAD package, (2007), "User manual,"Infolytica Corporation Ltd.
[10] Peter Balazovic and Roman Filka, (2011), "Sensorless PMSM Control for an H-axis Washing Machine Drive," Freescale Semiconductor.
[11] Bojoi, R. He, B. Rosa, F. et al., (2011), "Sensorless Direct Flux and Torque Control for Direct-drive Washing Machine Applications," IEEE in Energy Conversion Congress and Exposition (ECCE), pp. 347-354.
[12] Murray, A. Palma, M. and Husain, A. (2008), "Performance Comparison of Permanent Magnet Synchronous Motors and Controlled Induction Motors in Washing Machine Applications Using Sensorless Field Oriented Control," IEEE In Industry Applications Society Annual Meeting, IAS'08., pp. 1-6.